Applied Environmental Research
- RESEARCH FOR SUSTAINABLE PLANET -

Research Article

Exploring Google Earth Engine, Machine Learning, and GIS for Land Use Land Cover Change Detection in the Federal Capital Territory, Abuja, between 2014 and 2023

Akus Kingsley Okoduwa* **Chika Floyd Amaechi**

Department of Environmental Management and Toxicology, Faculty of Life Sciences, University of Benin, PMB 1154, Benin City, Nigeria

*Correspondence Email: akus.okoduwa@lifesci.uniben.edu

Abstract

This study aims to visualize various land use land cover (LULC) classes, estimate the net change in LULC types between the years 2014 and 2023, and use transition mapping to track LULC transitions within waterbody, vegetation, bareland, and buildup to better understand how land use types change from one another. Google Earth Engine (GEE), Random Forest (RF), and Geographic Information System (GIS) were used for LULC classification and change detection. The dataset employed for this study is Landsat-8 with 30 m resolution, and four land cover classes, which include waterbody, vegetation, bareland, and buildup, were classified for this study using RF. The training samples for each class were divided into two groups: 60% were used for LULC classification, and 40% were used for accuracy assessment. The overall accuracy (OA) for 2014 and 2023 was 91% and 92%, while the Koppa coefficient (KC) for 2014 and 2023 was 0.88% and 0.89% giving validation to the quality and reliability of this research. The result showed that between 2014 and 2023, waterbody increased from 27.56 km^2 to 36.67 km^2, vegetation cover decreased from 3,153.73 km^2 to 1,283.62 km^2, bareland increased from 3,660.74 km^2 to 4,845.30 km^2, and buildup area increased from 541.21 km^2 to 1,217.69 km^2. The transition results show that vegetation cover is being rapidly replaced by bareland and buildup. The results of this study are crucial for directing land use planning in Abuja and other developing regions of the world to enhance sustainable urban expansion. To help the government and policymakers support sustainable development, further research should be conducted to deepen the understanding of urban growth and its consequences.

ARTICLE HISTORY
Received: 20 Nov. 2023
Accepted: 25 May 2024
Published: 27 Jun. 2024

KEYWORDS
Google Earth Engine;
Random Forest;
GIS;
Land use Land cover;
Abuja

Introduction

Remotely sensed imagery is considered the most widely used data source for LULC mapping and land change monitoring; in particular, Landsat images are the most commonly used data [1]. The problem with remotely sensed imaging is the large volume of data that is produced when large areas are mapped for changes in LULC [2], making a user's personal computer inefficient and costly in terms of storage space and time [3]. This is where cloud-computing systems like GEE come in.

GEE is a computing platform capable of archiving a petabyte of geospatial data that is freely accessible and efficient for visualization and analysis [4]. What makes GEE more flexible is the fact that it allows the analysis of images on the platform itself with a script of code running on the code editor without downloading any local software [5]. In this way, users can easily access, select, and process large volumes of data for a large study area [6]. GEE and GIS have made it easier to track changes in LULC from the past to the present. GEE has also been employed in a variety of fields, including air quality monitoring [7], agriculture, forestry

https://doi.org/10.35762/AER.2024029

[8–9], and surface temperature monitoring [10], thus contributing to the growth of the scientific community.

The impact of changes in LULC results in a reduction in vegetation cover [11]. The loss in vegetation cover, in turn, leads to many other deleterious effects on the environment, such as loss of biodiversity, climate change, and pollution of other natural ecosystems [12]. Knowledge of LULC change is essential in urban and regional planning as well as natural resource planning [13]. Assessment of LULC change is required to understand rapid and uncontrolled urban growth along with economic and industrial development, especially in developing countries with intensified LULC changes [14].

The application of machine learning algorithms to remotely sensed images for LULC mapping has been attracting considerable attention [15]. The machine learning techniques have been categorized into two categories: supervised and unsupervised machine learning [16]. The supervised classification techniques include support vector machine (SVM), random forest (RF), maximum likelihood classifier (MLC), spectral angle mapper (SAM), fuzzy adaptive resonance theory-supervised predictive mapping (Fuzzy ARTMAP), Mahalanobis distance (MD), radial basis function (RBF), decision tree (DT), multilayer perception (MLP), naive Bayes (NB), and fuzzy logic [17–18].

The unsupervised classification techniques include the Affinity Propagation (AP) cluster algorithm, fuzzy c-means algorithms, K-means algorithm, and ISODATA (iterative self-organizing data) [19]. Each machine learning technique has different types of accuracy levels, and it has been reported that SVM and RF generally provide better accuracy as compared with the other traditional classifier techniques [20].

This study aims to estimate the net change in LULC classes between 2014 and 2023, visualize and quantify the spatial distribution, as well as use transition mapping to track LULC changes within waterbody, vegetation, bareland, and buildup classes.

Methodology

1) Study area

Abuja Municipal Area Council (AMAC), Bwari, Gwagwalada, Kuje, Kwali, and Abaji are the six area councils in Abuja. The total land area of these six councils is approximately 7,317 km^2 [21], with GPS coordinates of 9°5′ N and 7°32′ E. The city has both a rainy/wet and a hot/dry season. There is a short harmattan season, which is characterized by dry and dusty northeast trade winds sweeping through West Africa from the Sahara, resulting in chilly and dry weather conditions, particularly from November to early March. Rainfall patterns in the city are influenced by its location on the windward side of Jos and in the convergence zone, which receives regular rainfall during the monsoon season [22]. Daytime temperatures in the city range from 28°C to 40°C, while nighttime temperatures range from 12°C to 23°C [23].

2) Data source and data analysis

This study uses atmospherically corrected Landsat 8 Operational Landsat Imager and Thermal Infrared Sensor (OLI/TIRS) satellite imagery, which can be accessed through the GEE catalog. Landsat 8 data is available from 2013 till date, however, due to incomplete data for the year 2013 this study relied on data obtained for 2014 and 2023. Landsat 8 OLI/TIRS is considered a reliable satellite with open source status, featuring a spatial resolution of 30 meters and comprising eleven (11) bands. In the data analyses, seven (7) bands (SR_B1 to SR_B7) were employed for this study; various steps were conducted to extract information on LULC changes from the Landsat 8 OLI/TIRS imagery (Figure 2). Satellite imagery from 2014 and 2023, with cloud cover set to less than one percent to eliminate pixels that were contaminated by clouds was used for this research. To create a single image for each year, the acquired images were combined using a median filter.

For the purpose of classification, it is necessary to have training data to provide classification references for the classification algorithm. Additionally, there is validation data for accuracy assessment. The sample data collected for each LULC class was separated into 60% (for training RF classifier) and 40% (for validating the result). Each LULC training data point for 2014 consists of 115 points (waterbody), 115 points (vegetation), 112 points (bareland), 117 points (buildup), and 42, 48, 42, and 43 validation data points (Table 1). Each LULC training data point for 2023 consists of 115 points (waterbody), 115 points (vegetation), 112 points (bareland), 117 points (buildup), and 47, 41, 44, and 53 validation data points (Table 2). The data sampling was conducted using the GEE cloud computing software, which provides high-resolution time series images, allowing for data sampling to be adjusted to the target period of 2014 and 2023.

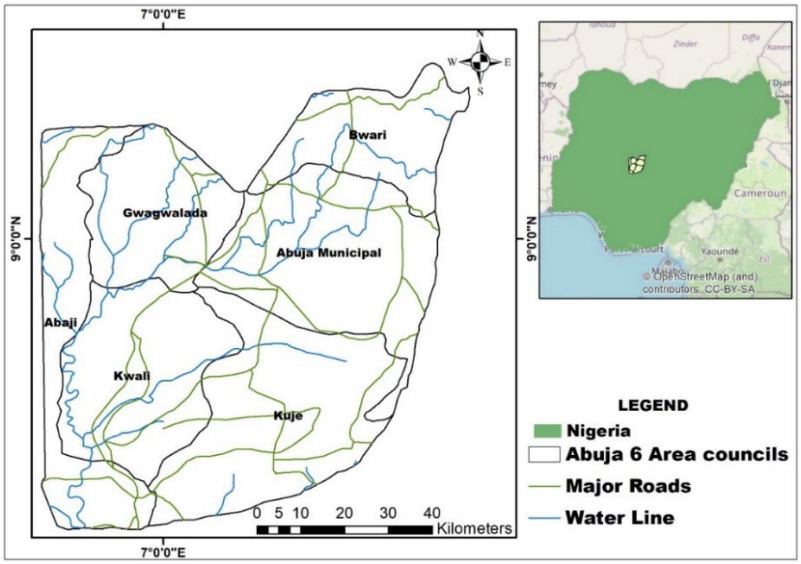

Figure 1 Map of FCT, Abuja.

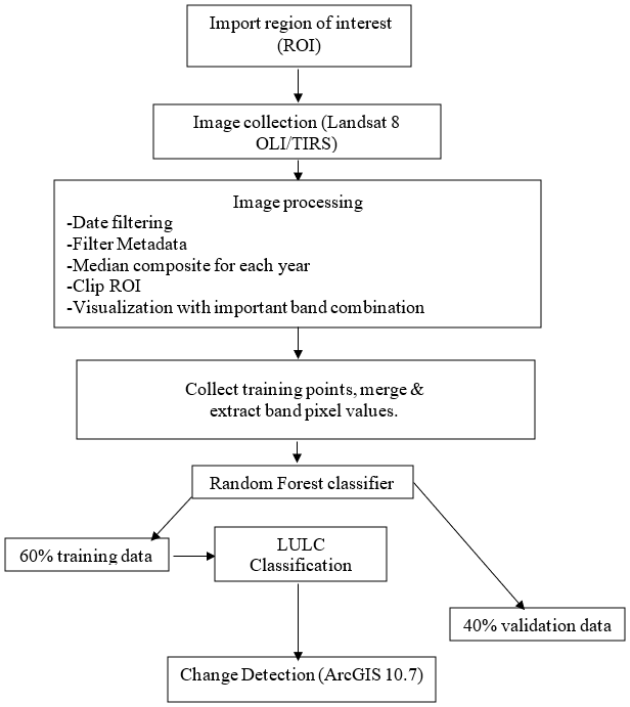

Figure 2 Research flowchart.

3) Random forest (RF)

The RF classifier is a machine-learning technique that uses multiple tree classifiers during LULC classification. To classify a land cover class, each tree classifier assigns a unit vote to the most common class in the tree. During the classification phase, each decision tree in the forest votes for the most popular land cover class. The RF final output is selected via a majority voting method, in which the class with the most votes across all trees is allocated to the land cover class. The decision to use RF in this study was based on previous research that demonstrated better performance of RF compared to other decision tree-based learning methods [24–26].

4) Accuracy assessment

The classification process for LULC often results in misclassification. Consumer's Accuracy (CA), Producer's Accuracy (PA), Overall Accuracy (OA), and Kappa Coefficient (KC), which were calculated from the training sample results in the Confusion Matrix, give validation to all LULC results [27]. A code script was used in GEE to evaluate each parameter's accuracy. The confusion matrix can provide information not only about classification errors but also about the errors produced. CA is a measure of commission errors that measures how accurately the classification reflects the actual conditions. PA measures omission errors, which measure how accurately LULC types can be classified, and OA compares the truth of each pixel classified using training data with validation data. Furthermore, KC is frequently employed to assess classification accuracy [5]. The following is the formula for accuracy assessments (Eq. 1–4).

$$\text{Consumer Accuracy} = \frac{\text{Number of correctly classified training samples in each class}}{\text{Number of training samples classified to that class}} \quad \text{(Eq. 1)}$$

$$\text{Producer Accuracy} = \frac{\text{Number of correctly classified training samples in each class}}{\text{Number of training samples in each class}} \quad \text{(Eq. 2)}$$

$$\text{Overall Accuracy} = \frac{\text{Number of correctly trained samples}}{\text{Number of total samples}} \quad \text{(Eq. 3)}$$

$$\text{Koppa Coefficint} = \frac{Overall\ Accuracy - \text{Estimated chance agreement}}{1 - \text{Estimated chance agreement}} \quad \text{(Eq. 4)}$$

Table 1 Confusion matrix for 2014 showing LULC class, description, correct and incorrect number of training samples

LULC Class	Description	Waterbody	Vegetation	Bareland	Buildup
Waterbody	Area covered by waterbody.	41	1	0	0
Vegetation	Areas dominated by trees and grasses.	0	45	3	0
Bareland	Non-vegetated barren (sand, rock, soil) areas.	0	1	35	6
Buildup	Impervious surface area including building materials, and asphalt.	0	0	5	38

Table 2 Confusion matrix for 2023 showing LULC class, description, correct and incorrect number of training samples

LULC Class	Description	Waterbody	Vegetation	Bareland	Buildup
Waterbody	Area covered by waterbody.	45	2	0	0
Vegetation	Areas dominated by trees and grasses.	1	39	0	1
Bareland	Non-vegetated barren (sand, rock, soil) areas.	0	0	39	5
Buildup	Impervious surface area including building materials, and asphalt.	0	0	6	48

5) Data analysis in ArcGIS

After classification in GEE, the LULC maps for 2014 and 2023 were imported into ArcGIS 10.7. The intersect tool was then utilized to calculate the geometric intersection of the two feature classes, generating a change detection map (Figure 5).

Results and discussion

1) Classification accuracy

Table 3 displays the results of LULC accuracy for the years 2014 and 2023 for CA, PA, OA, and KC. The OA and KC show that the LULC classifications had high accuracy ratings. 91% and 92%, respectively, were the OA for 2014 and 2023. Based on the corresponding confusion matrix data, the respective overall KC for the years 2014 and 2023 are 0.88% and 0.89%. This number indicates almost perfect agreement and validates this analysis.

Kappa accuracy is measured on a scale of 0 to 1, with 0 representing agreement equal to chance. 0.1 to 0.20 indicates moderate agreement. 0.21–0.40 = fair agreement. 0.41– 0.60 = reasonable agreement. Significant agreement = 0.61–0.80. 0.81–0.99 = nearly perfect agreement 1 = complete agreement [29].

2) Land use land cover analysis between 2014 and 2023

The results (Table 4 and Figure 3) show that in 2014, waterbody covered an area of 27.57 km^2 (0.37%), vegetation covered an area of 3,153.73 km^2 (42.71%), bareland covered an area of 3,660.74 km^2 (49.58%), and the buildup covered an area of 541.21 km^2 (7.33%). The vegetation cover was highly distributed in the southern region of Kuje, while the buildup was mostly distributed in the eastern part of Abuja Municipal. For 2023, the outcomes (Table 4 and Figure 4) convey that waterbody covered an area of 36.67 km^2 (0.50%), vegetation covered an area of 1,283.62 km^2 (17.39%), bareland covered an area of 4,845.30 km^2 (65.63%), and buildup covered an area of 1,217.69 km^2 (16.49%). The result (Table 4) also shows that from 2014 to 2023, waterbody increased by 9.10 km^2, vegetation decreased by 1,870.11 km^2, bareland increased by 1,184.57 km^2, and buildup area increased by 676.48 km^2. Based on this result, bareland is the next most changing land cover class, with vegetation being the most.

Vegetation loss occurred in Abuja Municipal, Gwagwalada, Abaji, and Kwali. Some parts of Bwari and Kuje also experienced vegetation loss. The vegetation loss experienced led to the huge availability of bareland between 2014 and 2023; buildup areas expanded continuously, as indicated in Figure 3 and Figure 4. The result showed an increase in waterbody, which is contrary to the result of [2], which showed that there was no increase or decrease in waterbody from 1987 to 2017. We could say that the increase in impervious surfaces and drainage systems must have caused water accumulation. This aligns with the results of [14], which reported an increase in waterbody in Abuja from 1987 to 2021.

Table 3 PA, CA, OA, and KC for all classified LULC type between 2014 and 2023

Class	2014		2023	
	PA (%)	CA (%)	PA (%)	CA (%)
Waterbody	98	100	96	98
Vegetation	94	96	95	95
Bareland	83	81	89	87
Buildup	88	86	89	89
Overall accuracy (%)	91		92	
Koppa accuracy (%)	0.88		0.89	

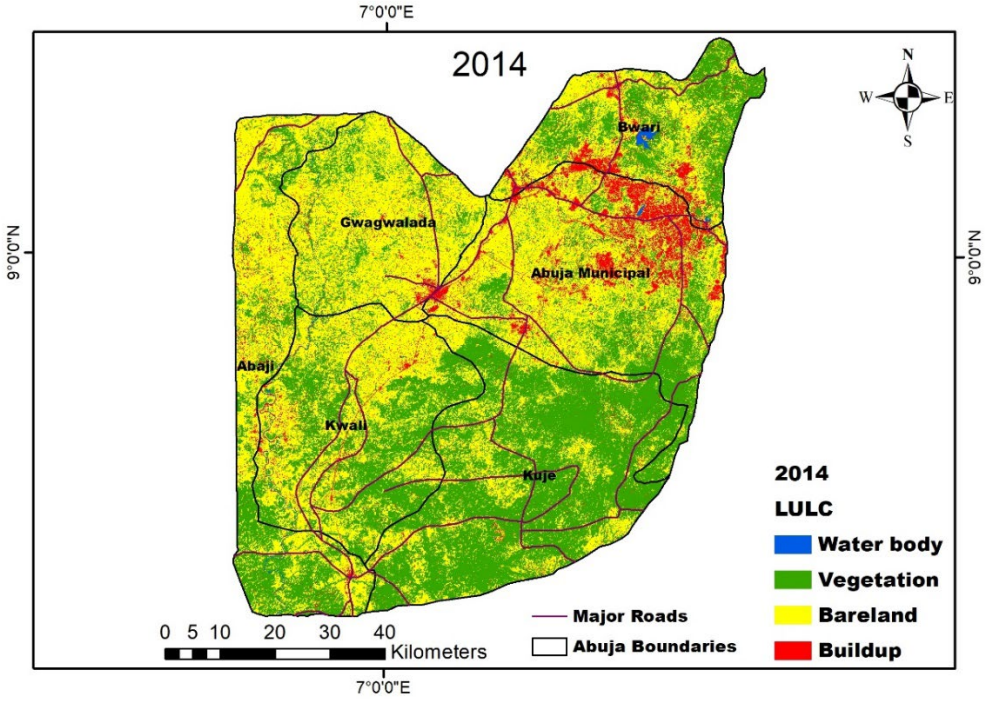

Figure 3 LULC for 2014.

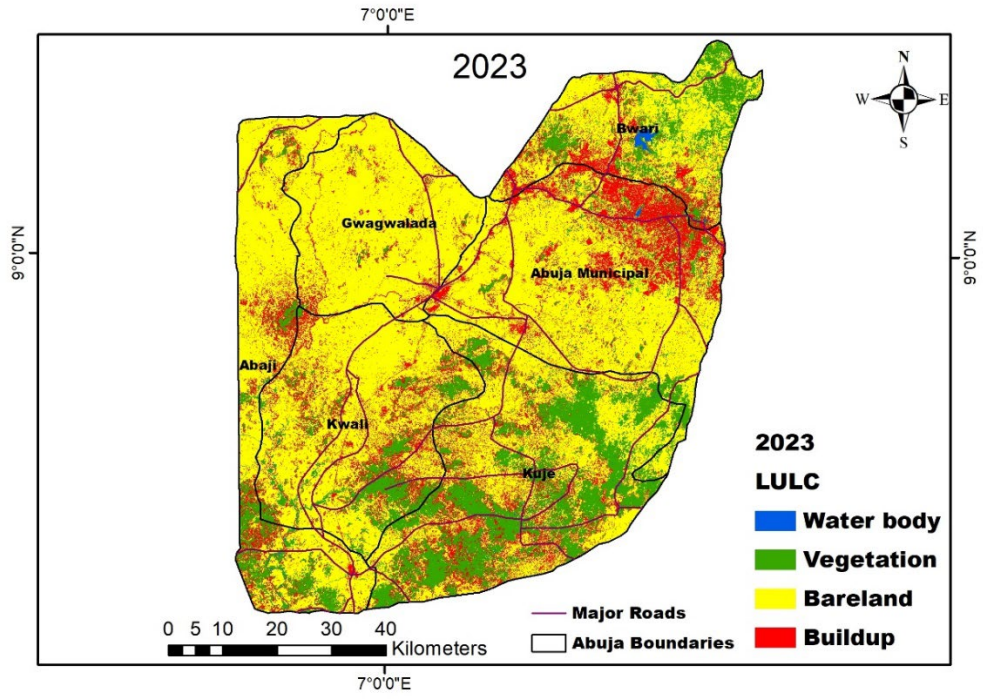

Figure 4 LULC for 2023.

Land use categories such as bareland and buildup have experienced significant expansion in their respective areas. In contrast, vegetation has shown a significant decline. It is plausible that the momentum of population growth constitutes one of the principal catalysts for the transformation of LULC. The aggregate population of Abuja amounted to 2.3 million individuals in 2014, which then escalated to 3.8 million in 2023 [30]. We posit that the surge in population and subsequent urbanization have generated a heightened demand for residential land and agricultural pursuits, thereby resulting in an increase in both the bareland and buildup areas, respectively. Based on the calculated statistics from the LULC images, the total area of vegetation was 3,153.73 km^2 in 2014, which decreased to 1,283.62 km^2 in 2023, which is a matter of great concern. According to Odjugo et al. [31], urbanization can lead to high demand for housing, which in turn can lead to deforestation. Many LULC changes, such as deforestation, may result in land degradation, and the conversion of vegetation to other land use types, such as bareland, can lead to loss of fertile soil [32].

As of 2015, Abuja was growing at a rate of at least 35% per year, keeping it as the fastest-growing metropolis on the African continent and one of the fastest-growing in the globe [33]. Since the buildup area in this study increased significantly (Table 4), the hypothesis is that as the number of households rises, there is a great demand for residential land, which causes the transformation of one land use type into another.

3) Change detection through transition mapping between 2014 and 2023

Figure 5 shows the transition map among various LULC classes. Table 5 indicates that between 2014 and 2023, 439.34 km^2 of bare land transitioned to buildup, 140.93 km^2 of bareland transitioned to vegetation, and 9.6 km^2 of bare land transitioned to waterbody. An area of 232.94 km^2 of buildup transitioned to bare land, 30.07 km^2 of buildup transitioned to vegetation, and 1.53 km^2 of buildup transitioned to waterbody. Additionally, 1,534.65 km^2 of vegetation transitioned to bareland, 486.28 km^2 of vegetation transitioned to buildup, and 130.79 km^2 of vegetation transitioned to waterbody. Lastly, 1.68 km^2 of waterbody transitioned to bareland, 12.63 km^2 of waterbody transitioned to buildup, and 1.57 km^2 of waterbody transitioned to vegetation.

Table 4 Calculated area of LULC class of Abuja in 2014 and 2023

LULC Class	Area (km^2) in % 2014	Area (km^2) in % 2023	Net change (km^2)
Waterbody	27.57 (0.37%)	36.67 (0.50%)	9.10
Vegetation	3,153.73 (42.71%)	1,283.62 (17.39%)	-1870.11
Bareland	3,660.74 (49.58%)	4,845.30 (65.63%)	1,184.57
Buildup	541.21 (7.33%)	1,217.69 (16.49%)	676.48

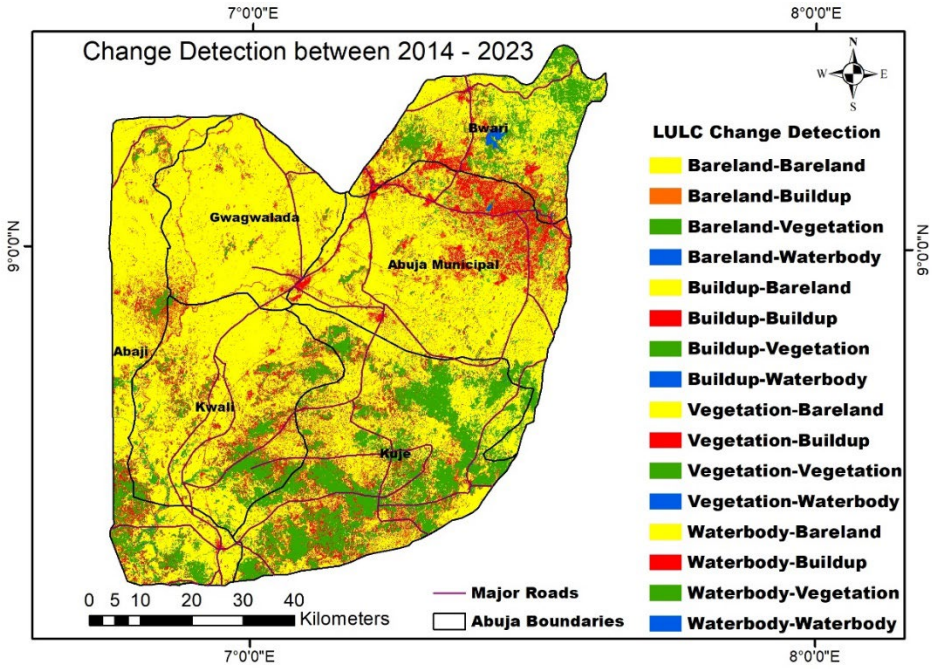

Figure 5 LULC change detection from 2014 – 2023.

Table 5 Change detection between 2014 and 2023

No.	LULC change detection	Changed area (km^2)
1	Bareland-bareland	3,056.08
2	Bareland-buildup	439.34
3	Bareland-vegetation	140.93
4	Bareland-waterbody	9.60
5	Buildup-bareland	232.94
6	Buildup-buildup	274.21
7	Buildup-vegetation	30.07
8	Buildup-waterbody	1.53
9	Vegetation-bareland	1,534.65
10	Vegetation-buildup	486.28
11	Vegetation-vegetation	1,105.37
12	Vegetation-waterbody	13.79
13	Waterbody-bareland	1.68
14	Waterbody-buildup	12.63
15	Waterbody-vegetation	1.57
16	Waterbody-waterbody	11.59
	Total	7,352.24

The findings of the transition mapping showed that buildup and bareland areas were expanding at the expense of vegetation cover. The results coincide with several previous studies [34–35], which observed buildup expansion at the expense of vegetation cover. Previous studies also highlights the loss of vegetation in developing regions due to urban expansion [34, 36–37], which is similar to the result of this research. In addition to the already rapid reduction of vegetation in Abuja, there was also an increase in barelands. This result is similar to [38] but contradicts that of [36], who reported a decrease in bareland in some parts of Abuja. An increase in bareland may be due to rapid increases in food and wood demands, in turn driving agricultural expansion and deforestation [2]. The expansion of bareland without afforestation has the potential to increase the risk of biodiversity loss. According to Moges et al. [39], there could also be a link between poor urban planning and the expansion of buildup areas at the expense of vegetation.

Conclusion

The utilization of the GEE platform for RS holds significant importance in offering a comprehensive depiction of the geographical scope of LULC change. This facet is indispensable for urban and regional planning, as well as environmental monitoring. in any region. In this study, LULC classes were classified using the GEE platform with RF algorithm, change detection was performed using ArcGIS 10.7. The OA for the years 2014 and 2023 amounted to 91% and 92%, respectively. The KC for the years 2014 and 2023, as deduced from the corresponding confusion matrix data, were determined to be 0.88% and 0.89%, respectively. The outcomes of this research indicate an increase in waterbody, bareland, and buildup areas while simultaneously witnessing a decline in vegetation coverage between the years 2014 and 2023. The change detection map shows rapid expansion of bareland and buildup areas at the expense of vegetation coverage. This result offers empirical support for the integration of RF with GEE and GIS as a valuable method for identifying changes in LULC. This productive methodology holds significance in terms of well-informed land use planning, to enhance environmental sustainability. This study adds to current research on LULC change detection to aid land use planning in developing nations around the world and to give the scientific community and policymakers information about the importance of sustainable urban expansion. To improve the accuracy of satellite image classification for LULC change detection, future research should integrate the normalized difference vegetation index to estimate vegetation density, the normalized difference built-up index to assess the extent of built-up areas, and the normalized difference water index to determine the extent of waterbody into the land use land cover classification.

References

[1] Wulder, M.A., Joanne, C.W., Thomas, R.L, Curtis, E.W., Alan, S.B., Warren, B.C., …, David P.R. The global Landsat archive: Status, consolidation, and direction. Remote Sensing of Environment, 2016, 185, 271–283.

[2] Enoguanbhor, E.C., Gollnow, F., Nielsen, J.O., Lakes, T., Walker, B.B. Land cover change in the Abuja City-Region, Nigeria: Integrating GIS and remotely sensed data to support land use planning. Sustainability, 2019, 11(5), 1313.

[3] Wan, B., Guo, Q., Fang, F., Su, Y., Wang, R. Mapping US urban extents from MODIS data using one-class classification method. Remote Sensing, 2015, 7(8), 10143–10163.

[4] Kumar, L., Mutanga, O. Remote sensing of above-ground biomass. Remote Sensing, 2017, 9(9), 935.

[5] Nasiri, V., Deljouei, A., Moradi, F., Sadeghi, S.M.M., Borz, S.A. Land use and land cover mapping using Sentinel-2, Landsat-8 satellite images, and Google Earth Engine: A comparison of two composition methods. Remote Sensing, 2022, 14(9), 1977.

[6] Gorelick, N., Hancher, M., Dixon, M., Ilyushchenko, S., Thau, D., Moore, R. Google Earth Engine: Planetary-scale geospatial analysis

for everyone. Remote Sensing of Environment, 2017, 202, 18–27.

[7] Okoduwa, KA., Amaechi, CF. monitoring and mapping of atmospheric concentration of carbon monoxide, sulphur dioxide, and nitrogen dioxide from 2019–2022 in Benin City, Southern Nigeria. Journal of Applied Sciences and Environmental Management, 2023, 27(12), 2715–2722.

[8] Tamiminia, H., Salehi, B., Mahdianpari, M., Quackenbush, L., Adeli, S., Brisco, B. Google Earth Engine for geo-big data applications: A meta-analysis and systematic review. ISPRS Journal of Photogrammetry and Remote Sensing, 2020, 164, 152–170.

[9] Kar, R., Reddy, G.O., Kumar, N., Singh, S.K. Monitoring spatio-temporal dynamics of urban and peri-urban landscape using remote sensing and GIS–A case study from Central India. The Egyptian Journal of Remote Sensing and Space Science, 2018, 21(3), 401–411.

[10] Ermida, S.L., Soares, P., Mantas, V., Gцttsche, F.M., Trigo, I.F. Google earth engine open-source code for land surface temperature estimation from the Landsat series. Remote Sensing, 2020, 12(9), 1471.

[11] Roy, P.S., Roy, A. Land use and land cover change in India: Aremote sensing & GIS prespective. Journal of the Indian Institute of Science, 2010, 90(4), 489–502.

[12] Wassie, S.B. Natural resource degradation tendencies in Ethiopia: A review. Environmental Systems Research, 2020, 9(1), 1–29.

[13] Hashem, N., Balakrishnan, P. Change analysis of land use/land cover and modelling urban growth in Greater Doha, Qatar. Annals of GIS, 2015, 21 (3), 233–247.

[14] Amaechi, C.F., Enuneku, A.A., Okhai, S.O., Okoduwa, K.A. Geospatial assessment of deforestation in federal capital territory Abuja, Nigeria from 1987 to 2021. Journal of Applied Sciences and Environmental Management, 2023, 27(11), 2457–2461.

[15] Aigbokhan, O.J., Ofordu, C.S., Essien, N.E., MbaEssien, N.C. Land cover accuracy assessment in Okitipupa, Ondo State, Nigeria; application of atmospheric correction and machine learning algorithms. Journal of Meteorology and Climate Science, 2022, 21(1), 29–53.

[16] Halder, A., Ghosh, A., Ghosh, S. Supervised and unsupervised landuse map generation from remotely sensed images using pant based systems. Applied Soft Computing, 2011, 11(8), 5770–5781.

[17] Ma, L., Liu, Y., Zhang, X., Ye, Y., Yin, G., Johnson, B.A. Deep learning in remote sensing applications: A meta-analysis and review. ISPRS Journal of Photogrammetry and Remote Sensing, 2019, 152, 166–177.

[18] Shih, H.C., Stow, D.A., Tsai, Y.H. Guidance on and comparison of machine learning classifiers for Landsat-based land cover and land use mapping. International Journal of Remote Sensing, 2019, 40(4), 1248–1274.

[19] Maxwell, A.E., Warner, T.A., Fang, F. Implementation of machine-learning classification in remote sensing: An applied review. International Journal of Remote Sensing, 2018, 39(9), 2784–2817.

[20] Carranza-Garcia, M., Garcia-Gutierrez, J., Riquelme, J.C.A framework for evaluating land use and land cover classification using convolutional neural networks. Remote Sensing, 2019, 11(3), 274.

[21] Ohiambe, E., Home, P.G., Coker, A.O., Sang, J. Assessing the surface rainwater harvesting potential for Abuja, Nigeria: A short-term projection. Nigerian Journal of Technological Development, 2019, 16(2), 63–70.

[22] Ekwe, M.C., Ibrahim, A.T., Balogun, I.A., Adedeji, O.I., Ekwe, D.O., Nom, J. Assessment of urban cooling island effects of Jabi Lake Reservoir, Abuja on its surrounding micro-climate using geospatial techniques, 2019, 19 (2), 1–10.

[23] Chibuike, E.M., Ibukun, A.O., Abbas, A., Kunda, J.J. Assessment of green parks cooling effect on Abuja urban microclimate using geo-spatial techniques. Remote Sensing Applications: Society and Environment, 2018, 11, 11–21.

[24] Jin, Y., Liu, X., Chen, Y., Liang, X. Land-cover mapping using Random Forest classification and incorporating NDVI time-series and texture: A case study of central Shandong. International Journal of Remote Sensing, 2018, 39(23), 8703–8723.

[25] Huynh-Cam, T.T., Chen, L.S., Le, H. Using decision trees and random forest algorithms to predict and determine factors contributing to first-year university students' learning performance. Algorithms, 2021, 14(11), 318.

[26] Phinzi, K., Ngetar, N.S., Pham, Q.B., Chakilu, G.G., Szaby, S. Understanding the role of training sample size in the uncertainty of high-resolution LULC mapping using random forest. Earth Science Informatics, 2023, 1–11.

[27] Cengiz A.V, Budak M, Ya mur N, Balɜik F. Comparison between random forest and support vector machine algorithms for LULC classification. International Journal of Engineering and Geosciences. 2023, 8(1), 1–0.

[28] Kadri, N., Jebari, S., Augusseau, X., Mahdhi, N., Lestrelin, G., Berndtsson, R. Analysis of four decades of land use and land cover change in semiarid Tunisia using Google Earth Engine. Remote Sensing, 2023, 15(13), 3257.

[29] Vilasan, R., kapse, V. Monitoring spatio-temporal dynamics of land use/land cover changes using remote sensing and GIS–A case study of Ernakulam District, India. Applied Ecology & Environmental Research, 2022, 20(4), 3353–3366.

[30] World Population Review. Abuja Population, 2022. [Online] Available from https://worldpopulation review.com/world-cities/abuja-population. [Accessed 1 October 2023].

[31] Odjugo, P.A., Enaruvbe, G.O., Isibor, H.O. Geospatial approach to spatio-temporal pattern of urban growth in Benin City, Nigeria. African Journal of Environmental Science and Technology, 2015, 9(3), 166–175.

[32] Rasool, R., Fayaz, A., ul Shafiq, M., Singh, H., Ahmed, P. Land use land cover change in Kashmir Himalaya: Linking remote sensing with an indicator based DPSIR approach. Ecological Indicators, 2021, 125, 107447.

[33] Musa, A., Jacob, O.N. Evaluation of challenges facing planning of special education in FCT, Abuja, Nigeria. European Journal of Humanities and Educational Advancements, 2021, 2(3), 31–37.

[34] Akpu, B., Tanko, A., Jeb, D., Dogo, B. Geospatial analysis of urban expansion and its impact on vegetation cover in Kaduna Metropolis, Nigeria. Asian Journal of Environment & Ecology, 2017, 3(2), 1–11.

[35] Owoeye, J.O., Ibitoye, O.A. Analysis of Akure urban land use change detection from remote imagery perspective. Urban Studies Research, 2016, 4673019.

[36] Ibrahim Mahmoud, M., Duker, A., Conrad, C., Thiel, M., Shaba Ahmad, H. Analysis of settlement expansion and urban growth modelling using geoinformation for assessing potential impacts of urbanization on climate in Abuja City, Nigeria. Remote Sensing, 2016, 8(3), 220.

[37] Hassan, M.M. Monitoring land use/land cover change, urban growth dynamics and landscape pattern analysis in five fastest urbanized cities in Bangladesh. Remote Sensing Applications: Society and Environment, 2017, 7, 69–83.

[38] Fanan, U., Dlama, K.I., Oluseyi, I.O. Urban expansion and vegetal cover loss in and around Nigerias Federal Capital City. Journal of Ecology and the Natural Environment, 2011, 3(1), 1–10.

[39] Moges, D.M., Bhat, H.G. An insight into land use and land cover changes and their impacts in Rib watershed, north-western highland Ethiopia. Land Degradation & Development, 2018, 29(10), 3317–3330.